

## Supplementary Information

# Enhanced CO<sub>2</sub> adsorption and selectives over N<sub>2</sub> and CH<sub>4</sub> in UiO-67 modified by loading CuO NPs using solvent exchange

Boyan Wang, Jing Zeng\* and Hanbing He\*

(School of Metallurgy and Environment, Central South University, Changsha 410083,  
China. E-mail: [213512168@csu.edu.cn](mailto:213512168@csu.edu.cn), [hehanbinghbb@163.com](mailto:hehanbinghbb@163.com) )

## Experimental

### 1. Materials

All reagents were commercially available and used as received. Zirconium chloride ( $\text{ZrCl}_4$ , 98%), Biphenyl-4,4'-dicarboxylic acid ( $\text{H}_2\text{BPDC}$ , 99%), 2,2'-Bipyridine-5,5'-dicarboxylic acid ( $\text{H}_2\text{bpydc}$ , 98%), Copper chloride dihydrate ( $\text{CuCl}_2$ , 99%), Benzoic Acid (BenAc, 99.5%), N,N-dimethylformamide (DMF, 99.5%), methanol (99.5%), ethanol (EtOH, 99.5%).

### 2. Synthesis of UiO-67

UiO-67 was synthesized according to a reported work. 0.36 g (1.542 mmol) of  $\text{ZrCl}_4$  and 7.53 g of benzoic acid were ultrasonically dissolved in 40 mL of DMF (solution A). Subsequently, 0.375 g (1.542 mmol) of  $\text{H}_2\text{BPDC}$  was fully dissolved in 20 mL of DMF by ultrasound (solution B). Finally, the solution A and solution B were fully mixed in a 100 mL Teflon-lined stainless-steel auto-clave reactor and placed in an oven at 120 °C for 24 h. After cooling to room temperature, the precipitates were isolated through centrifugation and washed with DMF and methanol for three times, respectively. The synthesized particles were dispersed in acetone and placed for 24 h at room temperature, followed by centrifugation. This treatment was repeated three times. The obtained particles were dried at 120 °C under vacuum for further procedures.

### 3. Synthesis of $\text{H}_2\text{bpydc-CuCl}_2$

$\text{H}_2\text{bpydc-CuCl}_2$  was synthesized according to the literature<sup>[23]</sup>. 60 mg (0.24 mmol) of  $\text{H}_2\text{bpydc}$  was dissolved in 20 mL of DMF (solution A) under 15 min stir. 45 mg (0.26 mmol) of  $\text{CuCl}_2$  was ultrasonically dissolved in 10 mL of DMF (solution B). Solution B was then added to solution A at 65 °C and stirring was continued at this temperature for 6 h to prepare a solution of  $\text{H}_2\text{bpydc-CuCl}_2$ .

### 4. Synthesis of $\text{CuO@UiO-67}$

90 mg of UiO-67 was ultrasonically dispersed in 10 mL DMF, the dispersion emulsion was added to the above  $\text{H}_2\text{bpydc-CuCl}_2$  solution and then stirred for 1 h at 60 °C. By centrifuging it, washed several times (three times at least) with DMF, Then, the prepared solid was isolated followed by three times washing with EtOH. The resulting solid after centrifugation was then dried under vacuum at 60 °C for 12h. The dried powder was placed in a 5%  $\text{H}_2/\text{Ar}$  gas stream, heated at 5 °C  $\text{min}^{-1}$  from room temperature to 250 °C, and held at 250 °C for 6 h. Then raised from room

temperature to 300 °C at a heating rate of 5 °C min<sup>-1</sup> under air atmosphere, it was also maintained at 300 °C for 3h.

## 5. Adsorption Experiments

CO<sub>2</sub>, CH<sub>4</sub>, and N<sub>2</sub> adsorption experiments were performed on a 3Flex surface characterization analyzer (Micromeritics, USA) at 273 and 298 K. The cuvette was placed in a circulating water bath to keep the adsorption temperature constant. The free space of the system was determined by dosing the helium gas. Prior to the measurements, 60-80 mg samples were degassed at 393 K for 12h. Gas adsorption isotherms were obtained at pressures from 0 to 100 kPa. Ultra-high purity CO<sub>2</sub> (99.99%), CH<sub>4</sub> (99.99%), and N<sub>2</sub> (99.99%) were used.

## 6. Calculations of the Adsorption Selectivity

In a mixture containing 1 and 2, the preferential adsorption selectivity of component 1 to component 2 can be formally defined as

$$S_{ads} = \frac{q_1/q_2}{p_1/p_2}$$

where  $q_1$  and  $q_2$  are the absolute loads. In all calculations below,  $S_{ads}$  are calculated based on the use of Myers and Prausnitz's Ideal Adsorption Solution Theory (IAST). These calculations were performed using a pure component isotherm fit of the absolute load.

## 7. Isothermic Heat of Adsorption

The isosteric heat of adsorption represents the strength of the interaction between adsorbent molecules and adsorbent lattice atoms and can be used to measure the energy inhomogeneity of a solid surface. The isosteric heat of adsorption can be calculated from the Clausius-Clapeyron equation as

$$Q_{st} = -RT^2 \left( \frac{\partial \ln P}{\partial T} \right)_{n_a}$$

where  $Q_{st}$  is the isosteric heat of adsorption (kJ/mol),  $P$  is the pressure (kPa),  $T$  is the temperature,  $R$  is the gas constant, and  $n_a$  is the adsorption amount (mmol/g).

## 8. Gas separation measurements

Breakthrough experiments on the gas separation performance of CuO@UiO-67 are carried out using a CO<sub>2</sub>/N<sub>2</sub> (15:85 v/v) gas mixture. 1g of activated CuO@UiO-67 is loaded into the instrumental multicomponent adsorption penetration profile analyzer BSD-MAB for testing at 298 K and 1 bar. Helium is used for initial blowdown of the

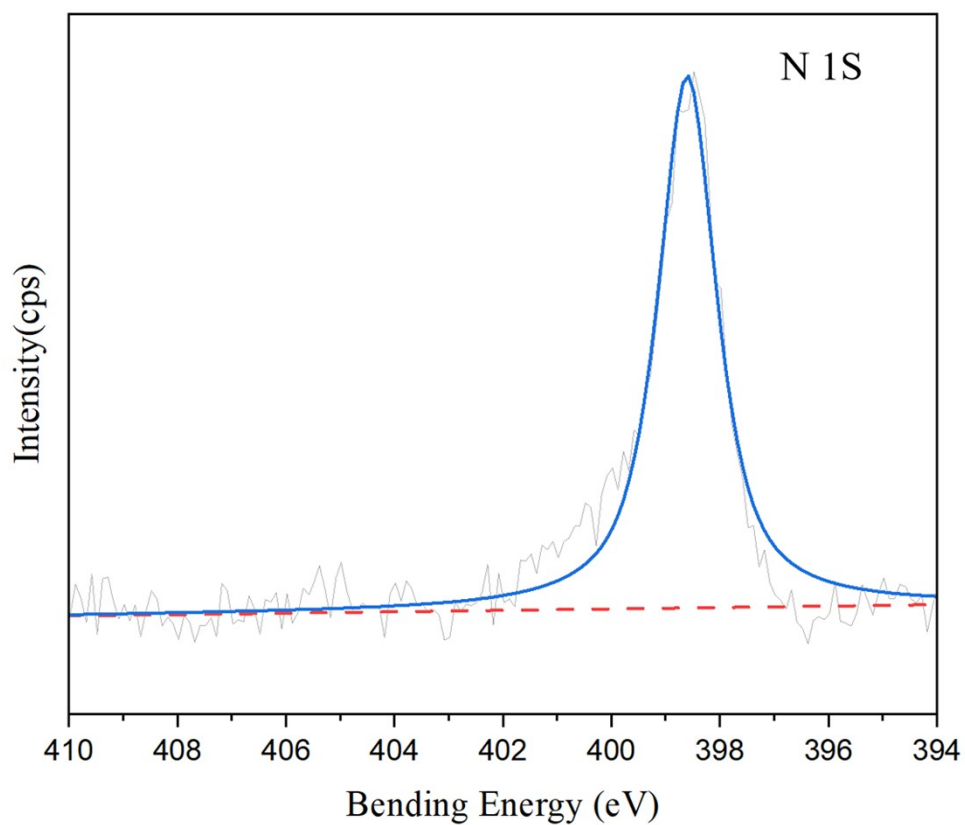
sample column, which is heated at 150 °C for 2 h for activation. The gas flow rate is 10 ml/min. The relative amount of gas passing through the column is monitored by a gas analysis system and the ion peaks are detected at  $m/z^+ = 15\ 44$  ( $\text{CO}_2$ ), 14 ( $\text{N}_2$ ), 40 (Ar).

#### 9. Cyclic Stability Test

The cyclic stability of  $\text{CO}_2$  was assessed using the TGA method on a thermogravimetric analyzer (PerkinElmer STA 8000, USA). The adsorbent underwent initial degassing at 120 °C under an argon atmosphere for 0.5 h, followed by cooling to 25 °C. At the onset of the first cycle, the gas flow was switched to  $\text{CO}_2$  for a 0.5 h adsorption phase. Subsequently, the  $\text{CO}_2$  atmosphere transitioned to an argon atmosphere, and the temperature was raised to 120 °C to desorb the adsorbent for 30 minutes. The material was then cooled to 25 °C, completing the first cycle. This entire process was repeated for a total of five cycles in the adsorption experiment. In each subsequent cycle, the steps of the first cycle were precisely replicated.

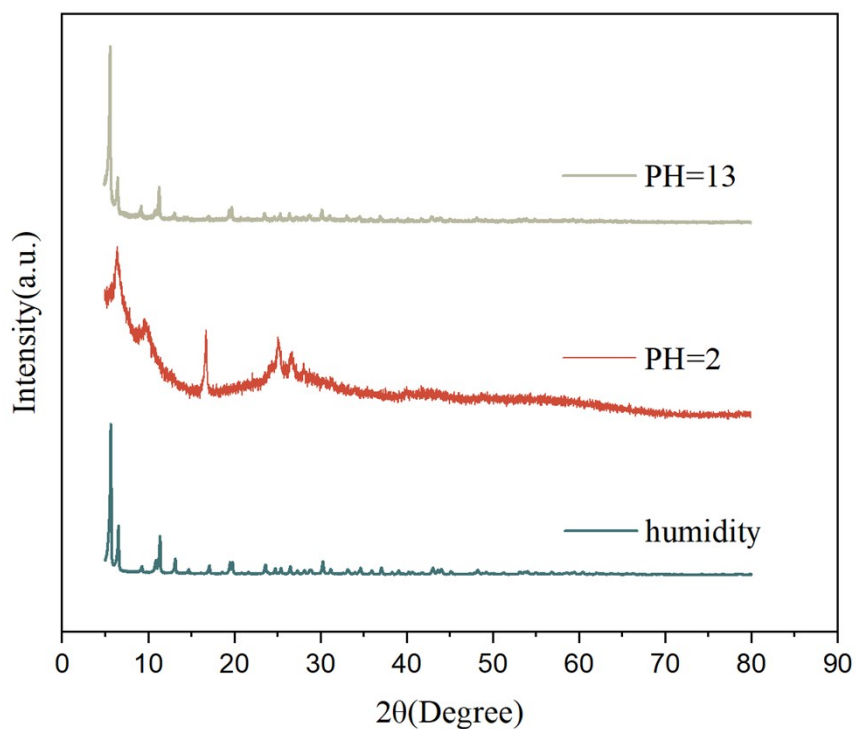
#### 10. Stability under humidity, acid and alkali condition

To assess the stability of the samples in acidic, alkaline, and humid environments, the specimens were subjected to exposure conditions: HCl with a pH of 2, NaOH solution with a pH of 13, and humid air with a relative humidity (RH) of 80%, each for 24 hours at ambient temperature. The stability was confirmed through PXRD analysis.



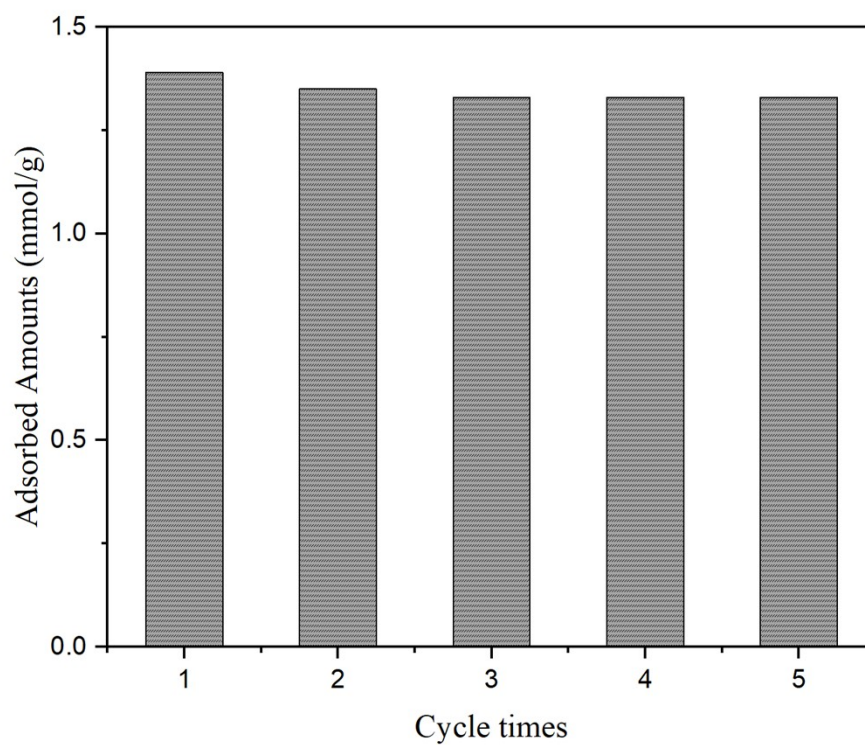
**Fig. S1.** Ex-situ high-resolution XPS spectra of bpydc@UiO-67.

Fig. S1 shows the XPS plot of bpydc@UiO-67 and we found that the peak position of substituted N (398.6 eV) is similar to that of H2bpydc (398.5 eV). The XPS analysis of H2bpydc-CuCl<sub>2</sub> into UiO-67 is shown in Fig. (Fig. 3b).



**Fig. S2.** XRD of CuO@UiO-67 after 24h at PH=2, PH=13 and 80% humidity, respectively.

Figure S2 shows the XRD of CuO@UiO-67 after placing it at PH=2, PH=13 and humidity of 80% for 24 h. From the figure, it can be noticed that the structure of CuO@UiO-67 has collapsed at PH=2, but it still maintains a good crystallinity at PH=13 and humidity of 80%. It indicates that CuO@UiO-67 has better alkali and water stability.



**Fig. S3.** Cyclic adsorption performance graph of CuO@UiO-67.

Figure S3 shows that after five cycles of adsorption, the adsorbed amount of CuO@UiO-67 only decreased by about 5%, which has a good cyclic stability.

Table S1. BET and CO<sub>2</sub> Adsorption Properties of CuO@UiO-67 and Selected MOFs Reported in the Published Literature at Room Temperature (298 K) and P = 1 bar

MOF	BET Surface areas (m <sup>2</sup> g <sup>-1</sup> )	CO <sub>2</sub> adsorption (mmol g <sup>-1</sup> ) at 298 K and 1 bar	ref
CuO@UiO-67	626	1.39	this work
UiO-67	1913	0.56	this work
MUT-1	28.17	0.97	1
ZIF-8	1567	0.70	2
(DMOF-1) ((Zn <sub>2</sub> (BDC) <sub>2</sub> (DABCO))	1161	1.60	3
Azo-DMOF-1	579.8	1.40	3
MOF-177	4508	0.80	4
PCN-68	5109	1.40	5
ZIF-70	1730	1.12	6
MOF-205	4460	0.75	7
CYCU-1	224	1.37	8
CYCU-2	297	1.17	8
SNU-9	259	1.25	9
MOF-5 (microwave synthesis)	2304	1.12	10
ZIF-8	1135	1.02	11
ZIF-100	600	0.96	12
UMCM-1	4034	0.91	10
MOF-5/IRMOF-1	1892	0.83	10
MOF-2	345	0.57	4
CALF-20	528	4.07	13
UTSA-120a	638	5.0	14
ZU-301		2.44	15

Table S2\_Selectivities of CO<sub>2</sub>/N<sub>2</sub> and CO<sub>2</sub>/CH<sub>4</sub> in some selected MOFs at 298k and a total pressure of 1 bar.

MOF	S <sub>CO<sub>2</sub>/N<sub>2</sub></sub> (CO <sub>2</sub> :N <sub>2</sub> )	S <sub>CO<sub>2</sub>/CH<sub>4</sub></sub> (CO <sub>2</sub> :CH <sub>4</sub> )	ref
CuO@UiO-67	55.6(15:85)	9.2(5:95)	this work
UiO-67	10.1(15:85)	0.4(5:95)	this work
UiO-67	11.8(16:84)	7.6(50:50)	17
Zr-BTDC	20.5(16:84)	17.2(50:50)	17
Zr-BFDC	58(16:84)	30.5(50:50)	17
BUT-10	22.9(15:85)	5.2(10:90)	18
BUT-11	43.1(15:85)	9.2(10:90)	18
Zn-MOF-74	87.8(15:85)		19
Mg-MOF-74	180(15:85)		19
Zn-paddlewheel MOF	36.7(15:85)	6.2(50:50)	20
Cu-BTC	20(15.6:84.4)	6.4(50:50)	21

ZIF-68	13(15:85)	3.5(50:50)	22
ZIF-69	24(15:85)	7(50:50)	22
UTSA-120a	600(15:85)		14
ZU-301	846(15:85)	111(50:50)	15
ZU-36-Ni	4200(15:85)	930(50:50)	16

## References

- [1].Alavijeh, R. K., Akhbari, K., & White, J. (2019). Solid–Liquid Conversion and Carbon Dioxide Storage in a Calcium-Based Metal–Organic Framework with Micro- and Nanoporous Channels. *Crystal Growth & Design*, 19(12), 7290–7297. <https://doi.org/10.1021/acs.cgd.9b01174>
- [2].Gadipelli, S., Travis, W., Zhou, W., & Guo, Z. (2014). A thermally derived and optimized structure from ZIF-8 with giant enhancement in CO<sub>2</sub> uptake. *Energy Environ. Sci.*, 7(7), 2232–2238. <https://doi.org/10.1039/C4EE01009D>
- [3].Xie, M.; Prasetya, N.; Ladewig, B. P. (2019). Systematic screening of DMOF-1 with NH<sub>2</sub>, NO<sub>2</sub>, Br and azobenzene functionalities for elucidation of carbon dioxide and nitrogen separation properties. *Inorg. Chem. Commun.* 108, 107512. <https://doi.org/10.1016/j.inoche.2019.107512>
- [4].Millward, A. R., & Yaghi, O. M. (2005). *Metal-Organic Frameworks with Exceptionally High Capacity for Storage of Carbon Dioxide at Room Temperature*. *J. Am. Chem. Soc.*, 127 (510), 17998–17999. <https://doi.org/10.1021/ja0570032?urlappend=%3Fref%3DPDF&jav=VoR&rel=cite-as>
- [5].Yuan, D., Zhao, D., Sun, D., & Zhou, H. (2010). An Isoreticular Series of Metal–Organic Frameworks with Dendritic Hexacarboxylate Ligands and Exceptionally High Gas-Uptake

Capacity. *Angewandte Chemie International Edition*, 49(31), 5357–5361.

<https://doi.org/10.1002/anie.201001009>

[6].Banerjee, R., Furukawa, H., Britt, D., Knobler, C., O’Keeffe, M., & Yaghi, O. M. (2009).

Control of Pore Size and Functionality in Isorecticular Zeolitic Imidazolate Frameworks and their Carbon Dioxide Selective Capture Properties. *Journal of the American Chemical Society*,

131(11), 3875–3877. <https://doi.org/10.1021/ja809459e>

[7].Sim, J., Yim, H., Ko, N., Choi, S. B., Oh, Y., Park, H. J., Park, S., & Kim, J. (2014). Gas

adsorption properties of highly porous metal–organic frameworks containing functionalized naphthalene dicarboxylate linkers. *Dalton Trans.*, 43(48), 18017–18024.

<https://doi.org/10.1039/C4DT02300E>

[8].Yeh, C.-T., Lin, W.-C., Lo, S.-H., Kao, C.-C., Lin, C.-H., & Yang, C.-C. (2012). Microwave

synthesis and gas sorption of calcium and strontium metal–organic frameworks with high

thermal stability. *CrystEngComm*, 14(4), 1219. <https://doi.org/10.1039/c2ce05875h>

[9].Park, H. J., & Suh, M. P. (2010). Stepwise and hysteretic sorption of N<sub>2</sub>, O<sub>2</sub>, CO<sub>2</sub>, and H<sub>2</sub> gases

in a porous metal–organic framework [Zn<sub>2</sub>(BPnDC)<sub>2</sub>(bpy)]. *Chem. Commun.*, 46(4), 610–612.

<https://doi.org/10.1039/B913067E>

[10].Zhao, Z., Li, Z., & Lin, Y. S. (2009). Adsorption and Diffusion of Carbon Dioxide on

Metal–Organic Framework (MOF-5). *Industrial & Engineering Chemistry Research*, 48(22),

10015–10020. <https://doi.org/10.1021/ie900665f>

[11].Yazaydin, A. Ö., Snurr, R. Q., Park, T.-H., Koh, K., Liu, J., LeVan, M. D., Benin, A. I.,

Jakubczak, P., Lanuza, M., Galloway, D. B., Low, J. J., & Willis, R. R. (2009). Screening of

Metal–Organic Frameworks for Carbon Dioxide Capture from Flue Gas Using a Combined

Experimental and Modeling Approach. *Journal of the American Chemical Society*, 131(51), 18198–18199. <https://doi.org/10.1021/ja9057234>

[12]. Wang, B., Côté, A. P., Furukawa, H., O’Keeffe, M., & Yaghi, O. M. (2008). Colossal cages in zeolitic imidazolate frameworks as selective carbon dioxide reservoirs. *Nature*, 453(7192), 207–211. <https://doi.org/10.1038/nature06900>

[13]. Lin, J.-B., Nguyen, T. T. T., Vaidhyanathan, R., Burner, J., Taylor, J. M., Durekova, H., Akhtar, F., Mah, R. K., Ghaffari-Nik, O., Marx, S., Fylstra, N., Iremonger, S. S., Dawson, K. W., Sarkar, P., Hovington, P., Rajendran, A., Woo, T. K., & Shimizu, G. K. H. (2021). A scalable metal-organic framework as a durable physisorbent for carbon dioxide capture. *Science*, 374(6574), 1464–1469. <https://doi.org/10.1126/science.abi7281>

[14]. Wen, H.-M., Liao, C., Li, L., Alsalmé, A., Allothman, Z., Krishna, R., Wu, H., Zhou, W., Hu, J., & Chen, B. (2019). A metal–organic framework with suitable pore size and dual functionalities for highly efficient post-combustion CO<sub>2</sub> capture. *Journal of Materials Chemistry A*, 7(7), 3128–3134. <https://doi.org/10.1039/C8TA11596F>

[15]. Yu, C., Ding, Q., Hu, J., Wang, Q., Cui, X., & Xing, H. (2021). Selective capture of carbon dioxide from humid gases over a wide temperature range using a robust metal–organic framework. *Chemical Engineering Journal*, 405, 126937. <https://doi.org/10.1016/j.cej.2020.126937>

[16]. Zhang, Z., Ding, Q., Peh, S. B., Zhao, D., Cui, J., Cui, X., & Xing, H. (2020). Mechano-assisted synthesis of an ultramicroporous metal–organic framework for trace CO<sub>2</sub> capture. *Chemical Communications*, 56(56), 7726–7729. <https://doi.org/10.1039/D0CC03196H>

- [17].Hu, J., Liu, Y., Liu, J., Gu, C., & Wu, D. (2018). Effects of incorporated oxygen and sulfur heteroatoms into ligands for CO<sub>2</sub>/N<sub>2</sub> and CO<sub>2</sub>/CH<sub>4</sub> separation in metal-organic frameworks: A molecular simulation study. *Fuel*, 226, 591–597. <https://doi.org/10.1016/j.fuel.2018.04.067>
- [18].Wang, B., Huang, H., Lv, X.-L., Xie, Y., Li, M., & Li, J.-R. (2014). Tuning CO<sub>2</sub> Selective Adsorption over N<sub>2</sub> and CH<sub>4</sub> in UiO-67 Analogues through Ligand Functionalization. *Inorganic Chemistry*, 53(17), 9254–9259. <https://doi.org/10.1021/ic5013473>
- [19].Xiang, S., He, Y., Zhang, Z., Wu, H., Zhou, W., Krishna, R., & Chen, B. (2012). Microporous metal-organic framework with potential for carbon dioxide capture at ambient conditions. *Nature Communications*, 3(1), 954. <https://doi.org/10.1038/ncomms1956>
- [20].Bae, Y.-S., Farha, O. K., Hupp, J. T., & Snurr, R. Q. (2009). Enhancement of CO<sub>2</sub>/N<sub>2</sub> selectivity in a metal-organic framework by cavity modification. *Journal of Materials Chemistry*, 19(15), 2131. <https://doi.org/10.1039/b900390h>
- [21].Yang, Q., Xue, C., Zhong, C., & Chen, J. (2007). Molecular simulation of separation of CO<sub>2</sub> from flue gases in CU-BTC metal-organic framework. *AIChE Journal*, 53(11), 2832–2840. <https://doi.org/10.1002/aic.11298>
- [22].Liu, B., & Smit, B. (2010). Molecular Simulation Studies of Separation of CO<sub>2</sub> /N<sub>2</sub> , CO<sub>2</sub> /CH<sub>4</sub> , and CH<sub>4</sub> /N<sub>2</sub> by ZIFs. *The Journal of Physical Chemistry C*, 114(18), 8515–8522. <https://doi.org/10.1021/jp101531m>
- [23].Liu, G., Zeller, M., Su, K., Pang, J., Ju, Z., Yuan, D., & Hong, M. (2016). Controlled Orthogonal Self-Assembly of Heterometal-Decorated Coordination Cages. *Chemistry - A European Journal*, 22(48), 17345–17350. <https://doi.org/10.1002/chem.201604264>